

## ExbB Protein in the Cytoplasmic Membrane of *Escherichia coli* Forms a Stable Oligomer<sup>†</sup>

Avijit Pramanik,<sup>\*,‡</sup> Fajun Zhang,<sup>§</sup> Heinz Schwarz,<sup>‡</sup> Frank Schreiber,<sup>§</sup> and Volkmar Braun<sup>‡</sup>

<sup>‡</sup>Max Planck Institute for Developmental Biology, Spemannstrasse 35, 72076 Tübingen, Germany, and <sup>§</sup>Institut für Angewandte Physik, Universität Tübingen, Auf der Morganstelle 10, 72076 Tübingen, Germany

Received July 19, 2010; Revised Manuscript Received August 26, 2010

**ABSTRACT:** In Gram-negative bacteria like *Escherichia coli* the ExbB–ExbD–TonB protein complex is anchored to the cytoplasmic membrane and is involved in energization of outer membrane transport. Outer membrane proteins catalyze energy-coupled transport of scarce nutrients. Energy is derived from the protonmotive force of the cytoplasmic membrane which is transferred through ExbB–ExbD–TonB to the outer membrane transporters. Earlier studies showed that ExbB is the most abundant protein of the ExbB–ExbD–TonB complex and stabilizes TonB and ExbD. To advance understanding of the role of ExbB in the membrane organization of the ExbB–ExbD–TonB complex, His-tagged ExbB was solubilized with decyl maltoside and purified to electrophoretic homogeneity. Its size and shape were determined by blue native gel electrophoresis, size exclusion chromatography, transmission electron microscopy, and small-angle X-ray scattering. Decyl maltoside bound to ExbB was quantified by the anthrone method that determines the sugar moiety of decyl maltoside. The results obtained with the four methods consistently indicated that isolated ExbB adopts a stable homooligomer with four to six monomers. We propose that the ExbB homooligomer forms a platform on which ExbD and TonB are assembled to form the energy-transducing complex in the cytoplasmic membrane.

Nutrients pass through the outer membrane of *Escherichia coli* by diffusion, facilitated diffusion, or energy-coupled transport. Diffusion is mediated by permanently open porin proteins, whereas energy-coupled transport is catalyzed by transport proteins consisting of a  $\beta$ -barrel with a pore that is tightly closed by a globular domain, called the plug. Such transport proteins import heme, ferric siderophores, vitamin B<sub>12</sub>, nickel, carbohydrates, or protein toxins called colicins (reviewed in refs (1–5)).

For transport, the substrates must be released from their high-affinity binding sites at the transport proteins, and the plug must move to open a channel. The energy required by these reactions is not generated in the outer membrane because the formation of a transmembrane potential is prevented by the pores through which compounds of  $\leq 700$  Da pass freely. Likewise, no energy-generating systems that form energy-rich compounds, i.e., ATP,<sup>1</sup> are found in the periplasm, the compartment between the outer membrane and the cytoplasmic membrane. The energy required for transport is rather derived from the electrochemical potential of the cytoplasmic membrane through the action of the proteins TonB, ExbB, and ExbD.

*E. coli* ExbB protein is predicted to have three transmembrane segments in the cytoplasmic membrane with the N-terminus in

the periplasm and the C-terminus in the cytoplasm (6). In contrast, the periplasmic TonB and ExbD proteins have a single N-terminal transmembrane domain through which they are anchored to the cytoplasmic membrane (7, 8). The C-terminal domain of TonB interacts with the outer membrane transport proteins, as revealed by genetic suppressor analysis, cross-linking between introduced cysteine residues, cross-linking with formaldehyde (1–5), and crystal structure determination of transport proteins with bound C-terminal fragments of TonB (9, 10). The three proteins presumably form a complex that reacts to the protonmotive force across the cytoplasmic membrane, thereby changing the complex conformation and in turn altering the structure of the outer membrane transport proteins such that the substrates are released from their binding sites and the pore in the  $\beta$ -barrel is opened for the substrates to enter the periplasm.

Radiolabeling of the proteins has revealed that more ExbB than ExbD and TonB is formed (11), and a careful determination of the protein concentrations in cells resulted in a 7:2:1 ratio for ExbB:ExbD:TonB (12). It is unclear whether these numbers reflect the stoichiometry of the proteins in the complex. These three proteins are expected to interact as shown by stabilization of TonB and ExbD by ExbB (11, 13). TonB forms dimers, as demonstrated *in vivo* in an assay in which TonB is fused to ToxR which in the dimeric form activates transcription of the *ctx* cholera toxin gene (14). Treatment of cells with formaldehyde did not reveal any larger complexes than dimers of TonB, TonB with ExbD, dimers of ExbB and ExbD, and dimers of ExbB with ExbD (15). Cysteine cross-linking of ExbB and TonB depends on an unimpaired response to the protonmotive force, which indicates a functionally relevant dimerization (16).

Since ExbB stabilizes TonB and ExbD and is synthesized in surplus over these two proteins, we hypothesized that ExbB is the scaffold for the entire complex. To investigate this hypothesis, we analyzed the oligomeric structure of ExbB using size exclusion

<sup>†</sup>This work was supported by grants from the Max Planck Society and the German Science Foundation (BR330/25-1).

\*To whom correspondence should be addressed. Phone: +497071601342. Fax: +497071601349. E-mail: avijit.pramanik@tuebingen.mpg.de.

<sup>1</sup>Abbreviations: ATP, adenosine triphosphate; *E. coli*, *Escherichia coli*; PCR, polymerase chain reaction; His<sub>6</sub>, hexahistidine; FLP, flippase recombinase; FRT, FLP recognition target; OD, optical density; IPTG, isopropyl  $\beta$ -D-thiogalactopyranoside; TBSSG, Tris-buffered saline with glycerol; Tris, 2-amino-2-(hydroxymethyl)propane-1,3-diol; PMSF, phenylmethanesulfonyl fluoride; DM, decyl maltoside; SDS, sodium dodecyl sulfate; PAGE, polyacrylamide gel electrophoresis; CD, circular dichroism; SAXS, small-angle X-ray scattering; CCD, charge-coupled device; GFP, green fluorescent protein.

chromatography, small-angle X-ray scattering, spectroscopic, and electron microscopic techniques.

## METHODS

**Cloning and in Vivo Functional Analysis.** The *exbB*–*exbD* genes were amplified from *E. coli* genomic DNA by PCR with the forward primer CCTGGAGATACACCATGGGTAATA and the reverse primer AGGGAATTCTACTTTACTTCTCGAATTGAGGATGCGACCATTTGGCGGTTTCTTCGCCGA. The amplified PCR products were cloned between the *Nco*I and *Eco*RI restriction sites of vector pET28a by restriction digestion, ligation, and transformation to generate pAP44, which encodes wild-type ExbB and ExbD with a C-terminal StrepII tag. The ribosomal binding site of *exbD* was optimized by inverse PCR of pAP44 with primers TTTTGTGCGACACGAACCGGATG and ATTACGCGCAGGATAAGGAGAATCCGATGGCAATGCA to generate pAP05, which was further subjected to inverse PCR with primers TTTTGTGCGACACGAACCGGATG and ATTACGCGCAGGACACCATCACCATCACCA-TACAGGATAAGGAGAATCCGATGG to generate pAP06, where the wild-type *E. coli* ExbB sequence is extended at the C-terminal end by eight amino acids (His<sub>6</sub>-Thr-Gly). Plasmid pAP06 was subjected to PCR with primers TGAGAATTCCG-GCTGCTAACAAAG and TCGGAATTCTCCTTATCTGTATG to yield pAP09, which removes *exbD* and encodes the His<sub>6</sub> affinity-tagged ExbB. The plasmids were introduced into *E. coli* C43  $\Delta$ *exbB* by transformation. *E. coli* C43  $\Delta$ *exbB* was constructed by P1 phage transduction from Keio collection strain *exbB::kan* of *E. coli* K-12 BW25113 and subsequent removal of the kanamycin resistance marker using the site-specific FLP/FRT recombination system (17). Resistance to kanamycin was used to select transformants. The correctness of the mutant constructs and clones was verified by PCR and DNA sequencing. Activity of ExbB *in vivo* was examined by placing filter paper disks soaked with various concentrations of colicin M and albomycin onto agar plates seeded with *E. coli* C43  $\Delta$ *exbB* transformed with the plasmid constructs expressing various combinations of ExbB alone or with ExbD.

**Protein Expression, Solubilization, and Purification.** Cells of *E. coli* C43  $\Delta$ *exbB* harboring plasmid pAP09 were grown overnight at 37 °C in 200 mL of LB medium (10 g of tryptone, 5 g of yeast extract, 10 g of NaCl per liter). The overnight culture was used to inoculate 5 L of LB medium. The culture was incubated with aeration at 37 °C to an OD<sub>600 nm</sub> of 0.8. Synthesis of ExbB was induced by adding 1 mM isopropyl  $\beta$ -D-thiogalactopyranoside (IPTG), and incubation was continued for 4 h at 30 °C. Cells were harvested by centrifugation, and the pellet was frozen at –80 °C until used. The cell pellet was suspended in 30 mL of TBSG (20 mM Tris, pH 8, 200 mM NaCl, 10% glycerol, 1 mM PMSF), and cells were disrupted by three passages through a French pressure cell at 15000 psi. Intact cells were removed by centrifugation at 4000g for 10 min, and the membrane fraction was pelleted by centrifugation at 186000g for 60 min, washed with TBSG supplemented with 0.5 M NaCl, and then suspended in 40 mL of TBSG with 1% decyl maltoside for 3 h at 4 °C. The insoluble membrane fraction was removed by centrifugation at 186000g for 60 min, and the supernatant was loaded onto a 20 mL nickel–nitrilotriacetate–agarose column equilibrated with TBSG containing 0.1% decyl maltoside (DM). The column was washed with 40 mL of TBSG/0.1% decyl maltoside, and the bound protein was eluted with a gradient of 0–200 mM imidazole in TBSG/0.1% decyl maltoside. The fractions were

monitored at A<sub>280nm</sub>. The peak fractions were pooled and concentrated to 7 mL with Amicon 50 kDa filters, loaded onto a Superdex 200 (26/60) column equilibrated with TBSG/0.1% decyl maltoside, and chromatographed with the same buffer. The collected fractions were concentrated and kept frozen at –80 °C until used.

**Protein Electrophoresis.** Proteins samples were regularly checked under denaturing reducing conditions by the standard Laemmli SDS–PAGE system (18). Blue native PAGE for native protein complexes were run on 4–16% bis-Tris native precast gels (Invitrogen) for 6 h at 200 V (19).

**Analytical Size Exclusion Chromatography.** Analytical size exclusion chromatography was performed on GE Healthcare 10/300 GL columns prepacked with Superose 6 or Superdex 200 matrix. Protein samples (200  $\mu$ L) were loaded onto the column pre-equilibrated with TBSG buffer with or without 0.1% decyl maltoside and were separated by running one column volume (24 mL) of the same buffer. Thyroglobulin (*M<sub>r</sub>* 669000), ferritin (*M<sub>r</sub>* 440000), catalase (*M<sub>r</sub>* 240000), conalbumin (*M<sub>r</sub>* 75000), bovine serum albumin (*M<sub>r</sub>* 67000), egg albumin (*M<sub>r</sub>* 45000), equine myoglobin (*M<sub>r</sub>* 18000), RNase A (*M<sub>r</sub>* 14000), and cytochrome *c* (*M<sub>r</sub>* 12000) were used as molecular mass standards.

**Circular Dichroism (CD) Spectroscopy.** CD spectra of purified ExbB in TBSG/0.1% decyl maltoside were recorded on a JASCO J-810 spectropolarimeter using a 1 mm path length quartz cell at 20 °C. The far-UV spectrum of the protein (0.6 mg mL<sup>–1</sup>) at wavelengths between 260 and 200 nm was recorded with a step resolution of 0.5 nm, a time constant of 1 s, a sensitivity of 10 mdeg, a scan speed of 200 nm min<sup>–1</sup>, and a spectral bandwidth of 5 nm. To reduce random error and noise, five scans were averaged for each spectrum. Background spectra were recorded from the TBSG/0.1% decyl maltoside buffer.

**Quantification of Detergent Bound to Protein.** The maltoside headgroup was used to quantify the detergent using the anthrone colorimetric method (20, 21). Briefly, 50  $\mu$ L each of standard decyl maltoside solutions, water, equilibration buffer, and various dilutions of protein samples in decyl maltoside were added to separate reaction tubes with 1.5 mL of 0.4% anthrone solution in 80% sulfuric acid. The closed tubes were heated for 20 min at 90 °C. After the tubes were cooled to room temperature, the absorbance at 622 nm was recorded. Standard curves were derived from the absorbance values plotted against known amounts of decyl maltoside. A linear trend line fit equation was derived from the standard curve, from which the total amounts of decyl maltoside present in the equilibration buffer and in protein samples were calculated. Detergent bound to protein was derived by subtracting the amount of free detergent present in equilibration buffer from the total detergent present in the protein sample.

**Small-Angle X-ray Scattering (SAXS).** SAXS data were collected at the ESRF (Grenoble, France) at beamline ID02 with a sample-to-detector distance of 2 m. The wavelength of the incoming beam was 0.108 nm (12 keV), covering a *q* range of 0.04–3.2 nm<sup>–1</sup> following the experimental procedure described in refs (22–24). The data were collected by a high-sensitivity fiber-optic-coupled CCD (FRLoN) detector placed in an evacuated flight tube. The protein samples were thoroughly dialyzed with a 50 kDa cutoff membrane against TBSG<sub>2</sub> (20 mM Tris, pH 8, 200 mM NaCl, 2% glycerol, 1 mM PMSF) buffer with 0.08% decyl maltoside. The protein solutions were loaded using a flow-through capillary cell of ~2 mm diameter with a wall thickness of approximately 50  $\mu$ m. No variation of SAXS profiles caused by radiation damage was observed during ten successive exposures

of 0.1 s. The incident and transmitted beam intensities were simultaneously recorded with each SAXS pattern with an exposure time of 0.3 s. The two-dimensional scattering intensity data were azimuthally averaged to obtain one-dimensional intensity profiles using an in-house software at the beamline (25). The recorded intensity,  $I$ , is expressed as a function of momentum transfer,  $q = 4\pi \sin \theta/\lambda$ , where  $2\theta$  denotes the scattering angle and  $\lambda$  denotes the wavelength of the incident beam (26). The absolute intensity was calibrated by the cross section of water as the standard using the equation:

$$I(q) = d\Sigma(q)/d\Omega_{\text{sample}} = \{I(q)_{\text{sample}}/I(0)_{\text{water}}\} \{d\Sigma/d\Omega_{\text{water}}\}$$

where  $I(q)_{\text{sample}}$  is the scattering intensity of the sample solution after correction and  $I(0)_{\text{water}}$  is the scattering intensity of water extrapolated to the origin.  $d\Sigma/d\Omega_{\text{water}} = 0.01632 \text{ cm}^{-1}$  is the constant scattering intensity of water at 293 K (27).

Scattering data were primarily analyzed using the ATSAS software package (28). At sufficient low- $q$  range ( $qR_g < 1.3$ ), the scattering intensity can be approximated by the Guinier law:  $\ln I(q) = \ln I(0) - (R_g^2 q^2)/3$ , where  $I(0)$  is the forward scattering and  $R_g$  is the radius of gyration (26, 29).

**Transmission Electron Microscopy.** Purified ExbB in TBSG/0.1% decyl maltoside at a concentration of  $5 \mu\text{g mL}^{-1}$  was spotted onto glow-discharged carbon-coated 400 mesh copper grids. The protein was allowed to stick to the grid for 2 min before blotting the excess buffer. After the grids were washed twice with 0.1% decyl maltoside in water, the grids were soaked in 1% uranyl acetate for 1 min. Excess uranyl acetate was carefully blotted, and the grids were air-dried before they were viewed under an FEI T12 microscope. Grids were examined at eucentric height at an acceleration voltage of 120 kV with a nominal magnification of 49000–120000 $\times$ . Micrographs were recorded digitally on a charge-coupled device mounted on the microscope. The micrographs were analyzed using ImageJ software (30).

## RESULTS

**In Vivo Activity of His-Tagged ExbB.** ExbB with an N- or C-terminal His<sub>6</sub> tag was cloned on plasmids and introduced into the *E. coli* C43  $\Delta\text{exbB}$  deletion mutant by transformation to test whether the recombinant protein restored ExbB-dependent activities. Transformants were tested for sensitivity to albomycin and colicin M which require the ExbB function for killing cells. N-Terminally His-tagged ExbB was inactive, presumably because the His tag interfered with translocation of the ExbB N-terminus across the cytoplasmic membrane (6), whereas wild-type ExbB and C-terminally His-tagged ExbB partially complemented *E. coli* C43  $\Delta\text{exbB}$ . Coexpression of ExbD along with wild-type ExbB or C-terminally His-tagged ExbB from the plasmid restored wild-type level sensitivity to albomycin and colicin M in *E. coli* C43  $\Delta\text{exbB}$ . The requirement for coexpression of ExbD was probably caused by a low level of chromosomally encoded ExbD in the mutant. Although the *exbB* gene was excised in frame and the common promoter of *exbB* *exbD* was retained, expression of ExbD was apparently reduced. The following studies were performed with functionally active C-terminally tagged ExbB.

**Overexpression, Solubilization, and Isolation of ExbB.** After induction of *exbB* transcription with IPTG in *E. coli* C43  $\Delta\text{exbB}$  pAP09 at 30 °C, the ExbB(His<sub>6</sub>) protein was enriched in the membrane fraction (Figure 1A, lane 5). The protein could be

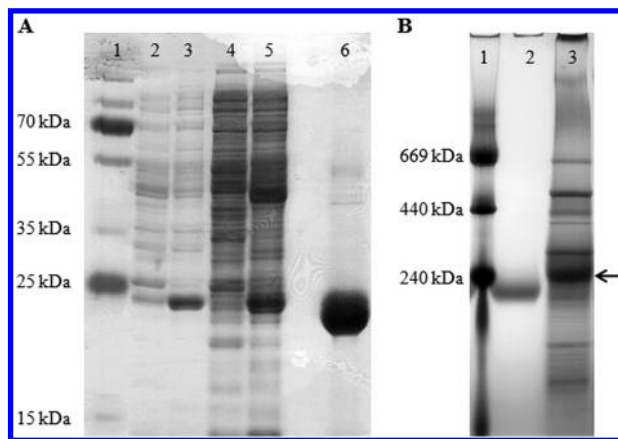


FIGURE 1: Expression and purification of ExbB. (A) Whole cell proteins and purified proteins were separated by SDS-PAGE and stained with Coomassie blue. Lanes: 1, standard denatured proteins; 2, uninduced cells; 3, induced, overexpressing cells; 4, cell lysate free of membranes; 5, membrane fraction; 6, purified ExbB. (B) Blue native electrophoresis stained with Coomassie blue. Lanes: 1, standard native proteins; 2, purified ExbB; 3, decyl maltoside soluble proteins from ExbB overexpressing cell membranes; the ExbB band is indicated by an arrow.

solubilized with 1% decyl maltoside, undecyl maltoside, octyl glucoside, cymal5, dodecylphosphocholine, or dodecyltrimethylamine *N*-oxide, whereas dodecyl maltoside, Triton X-100, tetradecyltrimethylamine *N*-oxide, decyldimethylphosphine oxide, and CHAPS poorly solubilized ExbB at or below 1% concentration (data not shown). Decyl maltoside was chosen for further experiments as it can easily be removed by dialysis and behaves neutral during purification procedures. ExbB solubilized with 1% decyl maltoside from the membrane fraction was chromatographed on a nickel–nitriloacetate–agarose column and was eluted between 100 and 150 mM imidazole in TBSG–0.1% decyl maltoside. Pooled fractions were passed through a preparation-grade Superdex 200 size exclusion column. The major elution peak at 280 nm contained a near homogeneous ExbB protein preparation (Figure 1A, lane 6, and Figure 1B, lane 2).

**Estimation of the Size of ExbB by Blue Native PAGE.** Blue native electrophoresis has recently gained much attention for the analysis of nondissociated protein complexes of the cytoplasm and membranes (31–33). We used this method to estimate the size of freshly prepared ExbB and to assess its stability during the purification process. The electrophoretic mobility of freshly solubilized ExbB was identical to catalase ( $M_r$  240000) used as marker protein, whereas purified ExbB showed a somewhat higher mobility (Figure 1B). We attribute the slight discrepancy in the size of freshly extracted and the purified sample to hydrophobic membrane components which stay bound to ExbB during electrophoresis. Recently, it has been shown that Coomassie blue replaces bound detergent on  $\alpha$ -helical membrane protein complexes during blue native electrophoresis which renders them a size approximately 1.8 times larger than that of a soluble protein (31). For the estimation of the size of ExbB we took this finding into account and arrived at a relative molecular mass of 110000–130000 which accounts for 4–4.8 monomers.

We also examined the native state of purified ExbB by CD spectroscopy. ExbB assumes a secondary structure rich in  $\alpha$ -helix as predicted by *in silico* analysis, which is expected due to its three transmembrane segments. The CD spectra showed prominent double negative signature peaks of  $\alpha$ -helix content of the purified protein (Figure 2), suggesting that purified ExbB retains a

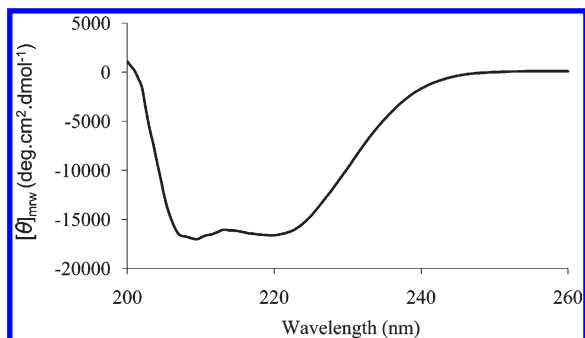


FIGURE 2: Circular dichroism of ExbB. The mean residue ellipticity of the ExbB–decyl maltoside sample is plotted against the applied wavelength (nm).

secondary structure consistent with that predicted for a transmembrane protein when in complex with decyl maltoside.

**Size Determination of ExbB in Detergent by Size Exclusion Chromatography.** The size of the purified protein detergent complex was determined by analytical size exclusion chromatography on Superdex 200 and Superose 6 columns, which differ somewhat in size exclusion limits and matrix. The columns were calibrated with proteins of known relative molecular mass, solubilized in TBSG buffer with and without 0.1% decyl maltoside. The elution position of the soluble standard proteins on Superdex 200 (10/300) was not altered by the presence of decyl maltoside, except for catalase and egg white albumin which eluted 0.01 column volumes later in the presence of decyl maltoside. Purified ExbB–DM complex eluted as a single peak between ferritin ( $M_r$  440000) and catalase ( $M_r$  240000) from both columns (Figure 3). A linear trend line fit equation was derived from the plot of log relative molecular mass versus  $V_e/V_t$  (elution volume/total column volume) of the standard proteins chromatographed without detergent. Detergent-solubilized ExbB eluted from the Superdex 200 column at 0.43  $V_e/V_t$  and from the Superose 6 column at 0.61  $V_e/V_t$  from which a relative molecular mass of 290000–310000 was derived. This calculated molecular mass for ExbB–DM is much larger than expected for monomeric ExbB with a molecular mass of 27268 indicating a homooligomeric state of ExbB.

Next we determined the hydrodynamic radius ( $R_h$ ) of the standard proteins chromatographed on the size exclusion column and compared it with the elution position of the ExbB–detergent complex. The ExbB eluted between native catalase ( $R_h = 5.3$  nm) and native ferritin ( $R_h = 6.2$  nm) corresponding to an  $R_h$  of 6.1 nm. For folded proteins of the size of ExbB (252 residues) the empirical value of  $R_h$  is 2.4 nm which extends to 5.2 nm on complete denaturation (34). The likely explanation for the larger  $R_h$  value is decyl maltoside bound to ExbB and oligomerization of ExbB.

**Electron Microscopic Estimation of the Shape and Size Distribution of ExbB.** The estimate of the relative molecular mass from size exclusion chromatography is based on the assumption that the shape and density of ExbB are equivalent to the used standard proteins. To gain knowledge of the actual size distribution and homogeneity of purified ExbB complex, the purified protein was stained with uranyl acetate and inspected under the electron microscope. Throughout the grid, nearly circular particle projections (Figure 4A) with a mean diameter of 10.5 nm were observed (Figure 4B). This finding supports the assumption that purified ExbB forms homogeneous homooligomers on which the relative molecular mass of ExbB was

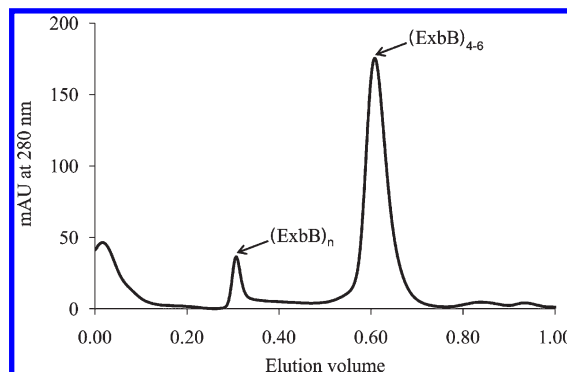


FIGURE 3: Analytical size exclusion chromatography of ExbB. ExbB in decyl maltoside was chromatographed on a Superose 6 (10/300) GL column with TBSG buffer. The elution was monitored by absorption at 280 nm. The elution volume is given as the fraction of the column volume. ExbB-containing elution peaks are marked by an arrow. The numbers outside parentheses indicate the oligomerization number;  $n$  = number not determined.

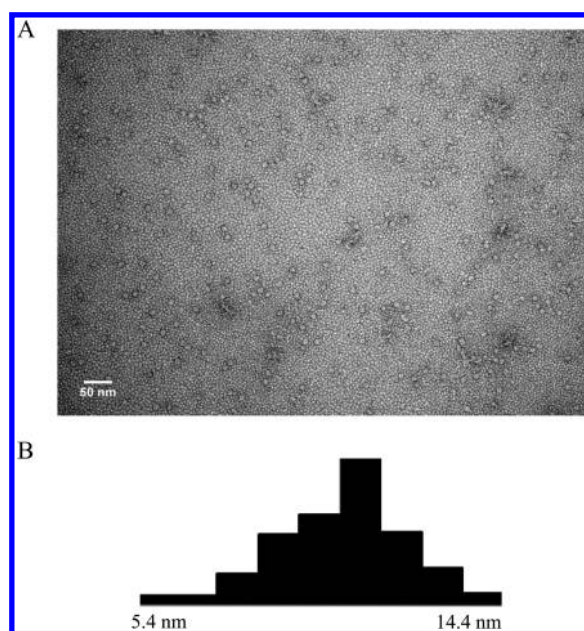


FIGURE 4: Electron microscopy of ExbB. (A) Detergent-solubilized ExbB sample negatively stained with uranyl acetate and viewed at 120000 $\times$  magnification. (B) Diameter distribution of uranyl acetate-stained ExbB particles. The plot represents 170 randomly picked particles, from which a mean diameter of 10.4 nm (standard deviation 1.6 nm) and a maximum diameter of 14.4 nm were derived.

calculated with the data obtained from size exclusion chromatography and blue native gel electrophoresis.

**Determination of Detergent Bound to ExbB.** For the estimation of the stoichiometry of the ExbB complex, it was necessary to determine the amount of detergent bound to the protein. We took advantage of the maltoside headgroup of decyl maltoside and measured the sugar content using the anthrone colorimetric method (20, 21). We observed a dose-dependent linear increase in absorbance at 10–120  $\mu$ g of decyl maltoside (data not shown). The protein content of the samples was quantified spectrophotometrically using the extinction coefficient of 20970 at 280 nm computed from the amino acid sequence with the ExPASy ProtParam webtool (35). The ExbB–decyl maltoside complex contained  $42 \pm 2\%$  (w/w) decyl maltoside, i.e., 38–44 molecules of decyl maltoside per ExbB molecule.

*Analysis of the Size and Shape of ExbB in Detergent Using Small-Angle X-ray Scattering (SAXS).* The results obtained from size exclusion chromatography and electron microscopy indicated that the isolated ExbB is oligomeric and contains bound decyl maltoside. To confirm the monodispersity and folding state of the purified protein in complex with detergent and to gain a scale-independent measure on the size and shape of the complex, we used SAXS. The individual scattering density of the protein and the detergent along with their mass contributions in the complex was used to determine the relative molecular mass of the complex.

We recorded the SAXS profile from purified ExbB in complex with decyl maltoside at six different protein concentrations ranging from 1.09 to 14.77 mg mL<sup>-1</sup> dissolved in TBSG<sub>2</sub> buffer with decyl maltoside. We have extensively dialyzed the protein samples against TBSG<sub>2</sub> buffer with 0.08% decyl maltoside, which is just below its critical micelle concentration (36), to reduce the signal noise from free micelle while keeping the protein in solution. The scattering of the dialyzing buffer was subtracted from the sample scattering. The experimental SAXS profiles of the samples are shown in Figure 5, where the recorded scattering intensity was plotted against the momentum transfer  $q$ . Guinier plots of  $\ln I(q)$  against  $q^2$ , with a  $q$  range satisfying the Guinier approximation  $qR_g < 1.3$  (29), gave a very good linear relationship throughout the measured protein concentration range (Figure 6). This suggested monodispersity and concentration-independent stability of the complex. The radius of gyration  $R_g$  and the forward intensity  $I(0)$  for each sample were calculated using the GNOM application (Table 1). The dynamic stability of the ExbB–decyl maltoside complex in solution at various concentrations was visually assessed from the Kratky plot of the SAXS profiles by plotting  $q^2I$  against  $q$  (Figure 7A). The plot assumes the typical bell shape, as expected for a globular particle (26, 37). In addition, the pair-distance distribution function,  $P(r)$  (Figure 7B), of the SAXS profiles was computed by indirect Fourier transformation using the GNOM application (38).  $P(r)$  is an inverse Fourier transform of scattering intensity and represents the summation of all the distances,  $r$ , between every pair of atoms within the protein and approaches zero at the maximum linear dimension of the particle ( $D_{\max}$ ). The  $P(r)$  distribution plots suggested a discoid shape for the sample particles with a maximum dimension  $D_{\max}$  of 11–15 nm (Table 1).

*Relative Molecular Mass of the Complex As Determined by SAXS.* The forward intensity  $I(0)$  in absolute intensity obtained from the Guinier analysis is related to the molecular mass as  $M_r = I(0)N_A/(c\nu^2\Delta\rho^2)$ , where  $N_A$  is the Avogadro number ( $6.022 \times 10^{23}$ ),  $c$  is the concentration of the protein complex in mg mL<sup>-1</sup>,  $\nu$  is the specific volume of the protein complex, and  $\Delta\rho$  is the difference of the electron density between the protein complex and the buffer solution. The  $I(0)$  was measured for the ExbB–decyl maltoside complex, whereas the protein concentration  $C_p$  was determined for ExbB without detergent using the theoretical extinction coefficient. The real concentration of the complex must therefore be corrected for the contribution of the detergent. The correction was made using the equation  $c = C_p/0.58$ , as the detergent fraction in the complex is 42% (w/w), where  $c$  is the concentration of ExbB–decyl maltoside and  $C_p$  is the concentration of ExbB without decyl maltoside. The partial specific volume of ExbB was calculated from the amino acid sequence of ExbB to be 0.7446 mL g<sup>-1</sup> using the SEDNTERP application based on the Cohn–Edsall method (39, 40). The partial specific volume of decyl maltoside is 0.8 mL g<sup>-1</sup> (41).

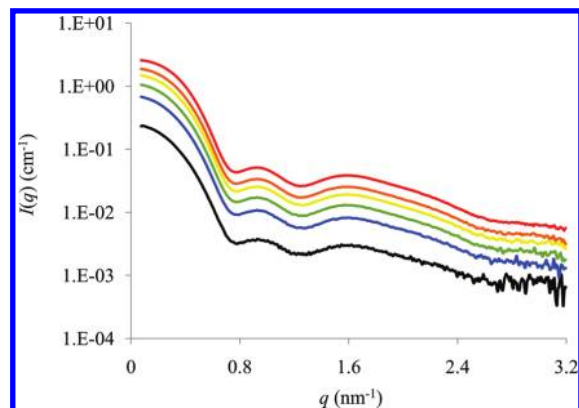


FIGURE 5: Solution scattering of ExbB. Experimental SAXS of ExbB–decyl maltoside samples are plotted as the momentum transfer,  $q$ , against the absolute intensity  $I(q)$  displayed on a logarithmic scale for better visibility. The  $q$  range covered is from 0.07 to 3.20 nm<sup>-1</sup>. Individual curves represent measured SAXS with ExbB at the following concentrations (mg mL<sup>-1</sup>): 1.09 (black), 3.22 (blue), 5.22 (green), 7.67 (yellow), 10.13 (orange), and 14.77 (red).

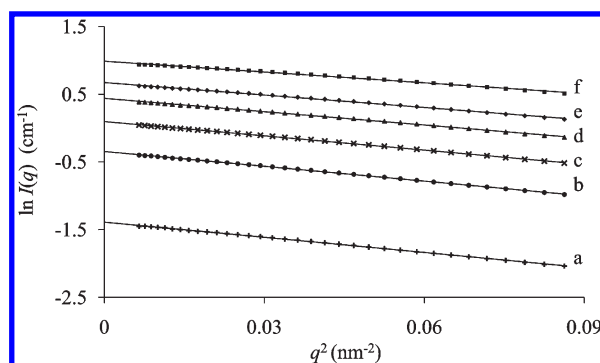


FIGURE 6: Guinier plots for SAXS data on ExbB samples. The natural logarithm of  $I(q)$  was plotted against the  $q^2$  within a  $q$  range of 0.08–0.29, which is valid in the Guinier approximation of  $R_g < 4.5$  nm. Individual data points were determined at protein concentrations (mg mL<sup>-1</sup>) of (a) 1.09, (b) 3.22, (c) 5.22, (d) 7.67, (e) 10.13, and (f) 14.77 and fitted to a linear trend line.

The specific volume of the complex,  $\nu = 0.768$  mL g<sup>-1</sup>, was calculated from the mass fractions of decyl maltoside and ExbB in the complex. The electron scattering density  $\rho$  was calculated for decyl maltoside, ExbB, and solvent (2% glycerol in water) using macros developed by the NIST center for neutron scattering research (42) and Irena SAS macros (43). The difference in electron scattering density ( $\Delta\rho$ ) between the solvent and the protein/detergent complex was calculated to be  $2.431 \times 10^{10}$  cm<sup>-2</sup>. The relative molecular mass of the complex was calculated directly for each SAXS profile to be 194000–230000 (Table 1). Taking into account the mass contribution of the detergent and the molecular mass of ExbB, the complex consists of four to five monomers.

## DISCUSSION

Energy-coupled transport across the outer membrane involves energy generation in the cytoplasmic membrane, where the ExbB–ExbD–TonB protein complex responds in an unknown way to the energized state of the cytoplasmic membrane and transfer energy from the cytoplasmic membrane to the transport proteins in the outer membrane. Response of the TonB structure to energization has been demonstrated (8). To understand this energy transduction process, knowledge of the structure of this

Table 1: SAXS-Derived Parameters of the ExbB–Detergent Complex<sup>a</sup>

protein (mg mL <sup>-1</sup> )	$R_g$ (nm)	$I(0)/C_{\text{complex}}$ (cm <sup>2</sup> ·mg <sup>-1</sup> )	$D_{\text{max}}$ (nm)	$M_r$ , ExbB–DM	$M_r$ , ExbB	no. of monomers
1.09	4.71	0.133	15	229821	133296	4.89
3.22	4.62	0.128	12.5	220320	127786	4.69
5.22	4.58	0.123	12	213284	123705	4.54
7.67	4.53	0.121	12	208765	121084	4.44
10.13	4.48	0.117	11.5	202184	117267	4.30
14.77	4.35	0.112	11	193552	112260	4.12
at infinite dilution:		0.133		229255	132968	4.88

<sup>a</sup>The radius of gyration ( $R_g$ ), the forward scattering intensity [ $I(0)$ ], and the maximum dimension ( $D_{\text{max}}$ ) were calculated using GNOM. The concentration of the protein–detergent complex ( $C_{\text{complex}}$ ) was calculated from the sample absorbance at 280 nm for protein and considering the detergent fraction. The relative molecular mass of the ExbB with bound detergent and without detergent was determined as described in the Methods section. The number of monomers derived from the calculated molecular mass of 27268 for ExbB.

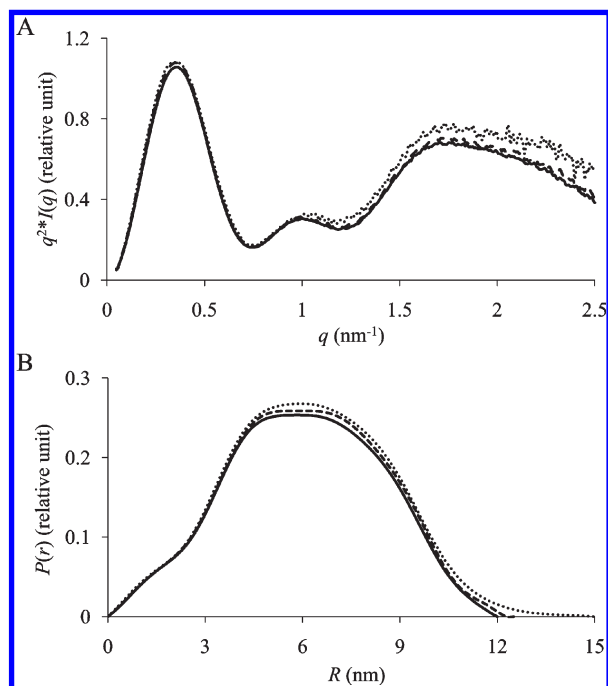


FIGURE 7: ExbB shape parameters derived from SAXS profiles. (A) Kratky plot of detergent-solubilized ExbB. Experimental solution SAXS intensity  $I(q)$  of ExbB samples was normalized for protein concentration to visually compare the Kratky plot for ExbB samples at concentrations (mg mL<sup>-1</sup>) of 1.09 (...), 3.22 (----), and 5.22 (—). (B)  $P(r)$  distribution functions for ExbB. The interatomic distance distribution was computed using GNOM on experimental SAXS profiles at ExbB protein concentrations (mg mL<sup>-1</sup>) of 1.09 (···), 3.22 (---), and 5.22 (—), and a  $D_{\text{max}}$  of 12–15 nm was obtained.

protein complex is essential. In this work, we focused on ExbB since it is the predominantly expressed protein of the complex (11, 13).

For this study we constructed ExbB His-tagged at the C-terminus for purification that was active in energy-dependent killing of cells by albomycin and colicin M. It could be over-expressed without harmful effects on host cells. ExbB was successfully solubilized and purified from the membrane fraction. SDS–PAGE revealed no TonB and no ExbD in purified ExbB. The chromosomal *exbB* deletion strain with reduced synthesis of ExbD was used for transformation with plasmid-encoded *exbB* to isolate ExbB. Natural synthesis of TonB is much lower than ExbB. Furthermore, lack of stoichiometric amounts of ExbB, ExbD, and TonB may have reduced the stability of ExbD and TonB. In addition, it is likely that the *in vivo* complex of the three proteins dissociated during solubilization in 1% decyl maltoside and only ExbB formed a stable complex. ExbB–decyl maltoside

chromatographed as a single peak on Superose 6 and Superdex 200 columns at a position which corresponded to a relative molecular mass of  $300000 \pm 10000$  and a hydrodynamic radius of 6.1 nm. The standard proteins used to calibrate the columns contained no or negligible amounts of bound detergent, whereas for ExbB a detergent content of 42% (w/w) was determined. For the calculation of the relative molecular mass of ExbB oligomer without detergent, the detergent content was subtracted, which resulted in a relative molecular mass of 185000, which is probably an overestimation as the average density of proteins (1.4 g mL<sup>-1</sup>) is higher than that of the detergent decyl maltoside (1.25 g mL<sup>-1</sup>) (41). The hydrodynamic radius is the more relevant property in size exclusion chromatography. A protein–detergent complex of hydrodynamic radius of 6.1 nm would have a lower relative molecular mass than for a protein with identical  $R_h$ . The number of 6.5 monomers per oligomer is thus somewhat too high but still in the range of the numbers derived from SAXS and electron microscopy.

In blue native electrophoresis purified ExbB migrated as a protein with a molecular mass of 210000. Blue native electrophoresis is a reliable method for the analysis of protein complexes with respect to composition, oligomeric state, and relative molecular mass. For the membrane protein complexes, it was shown that Coomassie brilliant blue replaces the detergent dodecyl maltoside during blue native gel electrophoresis (31). Empirical correction for the Coomassie dye bound to ExbB by the conversion factor 1.8 (31) resulted in 4–4.8 ExbB monomers per ExbB oligomer.

In a proteome survey of *E. coli* cells by blue native electrophoresis, denaturing electrophoresis, and mass spectrometry, multimeric ExbB was identified among 256 homomultimers of the entire proteome (33) and among 156 membrane proteins (32). A recent study of *E. coli* ExbB by analytical ultracentrifugation sedimentation velocity indicated a globular compact particle which, however, was monomeric (44). In contrast to our study, ExbB was solubilized with 3% dodecyl maltoside, whereas we used 1% decyl maltoside for solubilization and 0.1% decyl maltoside for the further studies. With long exposure of 2% dodecyl maltoside we also observed dissociation of oligomeric ExbB into smaller subunits. Our observation on purified ExbB by size exclusion chromatography and blue native electrophoresis along with the  $\alpha$ -helix-rich signal recorded in CD spectroscopy strongly suggests that the purified ExbB oligomeric complex represents the native structure that in the isolated form is oligomeric with four to six monomers.

To gain additional and independent information on the relative molecular mass of ExbB oligomer with bound detergent,

we used SAXS. This method relies on electron density contrast and can be measured on an absolute scale. To rule out possible concentration-dependent dynamic oligomerization of ExbB, SAXS data were collected at protein concentrations of 1.09–14.77 mg mL<sup>-1</sup>. The  $P(r)$  distribution plot and the Kratky plot (Figure 7) derived from all measured ExbB concentrations were superimposable at low  $q$  values, which suggested a stable complex of defined size and shape. At lower protein concentrations,  $R_g$  and  $D_{max}$  were progressively higher (Table 1). The SAXS data confirmed the homogeneity and dynamic stability of the sample and suggested a compact folded particle with an oblate to discoid shape for which a radius of gyration of 4.35–4.71 nm was calculated. This value is consistent with the hydrodynamic radius of 6.1 nm derived from size exclusion chromatography and a mean radius of 5.25 nm deduced from electron microscopy. The SAXS data reveal for the ExbB–decyl maltoside complex a relative molecular mass of 194000–230000. Here a relative molecular mass of 230000 refers to an infinitely dilute solution, which after correction for the bound detergent results in an estimate of 4.9 monomers per ExbB oligomer. A quantitative comparison of the data obtained with the four methods would require knowledge of the shape of ExbB. Nevertheless, observations from all of the applied experiments are largely consistent with the conclusion that ExbB–decyl maltoside forms a stable complex and assume an oblate to discoid shape, presumably with a detergent belt around the hydrophobic surface through which ExbB is inserted in the cytoplasmic membrane.

The number of four to six ExbB monomers in the stable oligomeric state determined in this work is smaller than suggested from the cellular content of the ExbB, ExbD, and TonB proteins which were found in a 7:2:1 ratio (12). Whether this ratio reflects the stoichiometry of the entire complex or includes fractions of free ExbB not bound to the complex is not known. Cross-linking studies with formaldehyde have identified homodimers of ExbB, ExbD, and TonB and heterodimers of TonB with ExbD and ExbB with ExbD (12, 15, 16). Larger ExbB oligomers were not cross-linked, possibly because of the low yield of cross-linked products which complicates identification of complexes larger than dimers. TonB homodimer formation has also been shown for the fusion protein of TonB with the DNA-binding domain of the ToxR transcriptional activator which is only active as a dimer (14). If TonB in the ExbB–ExbD–TonB complex is in the dimer form and the ratio of 7:2:1 applies, the complex would contain 14 ExbB monomers. During initial ExbB assembly the natural surplus of ExbB over ExbD and TonB most likely results in binding of ExbB monomers to each other without participation of ExbD and TonB. The oligomer we found may therefore form the foundation upon which the full complex is built by addition of ExbD, TonB, and additional ExbB monomers resulting in a biologically functional complex which may have a 7:2:1 or 14:4:2 stoichiometry.

*E. coli* contains two other systems that use the protonmotive force to carry out a mechanical function similar to that of ExbB–ExbD–TonB. The Tol system acts similarly to the Ton system (45). The proteins TolQ and TolR exhibit sequence similarities to ExbB and ExbD, respectively (46), and TolQ–TolR has the same transmembrane topology as ExbB–ExbD (6, 47). TolQ and TolR can even partially replace the functions of ExbB and ExbD (48). TolA, the functional homologue of TonB, differs in sequence, but the N-terminal membrane-anchored portion fused to an N-terminally truncated TonB yields a

functional TonB (49). It is assumed that TolA, TolQ, and TolR form a complex in the cytoplasmic membrane similar to that of TonB, ExbB, and ExbD. The size of this Tol complex has not been determined, but the proteins have been found in the ratios TolR:TolA 2:1 and TolQ:TolR 3:1 (45, 50). A probable TolQ:TolR:TolA stoichiometry of 4:2:1 has been proposed (45), with TolQ, like its homologue ExbB, as the most prominent protein (11, 13).

The second system similar to the Exb–Ton system is formed by the MotA and MotB proteins which in the cytoplasmic membrane build the stator of the flagellar motor driven by the protonmotive force. MotA shows sequence similarities to ExbB and TolQ, and MotB to ExbD and TolR; a homologue of TonB and TolA is lacking. Coexpressed MotA and MotB in detergent have been isolated and chromatographed on a size exclusion column. Compared with the elution of soluble standard proteins, the MotAB complex eluted at a position corresponding to a relative molecular mass of 300000. To determine the ratio of MotA and MotB, the proteins were labeled with [<sup>35</sup>S]methionine and separated by gel electrophoresis, and the radioactivity was counted. The MotA:MotB ratio was 2:1, and a MotA<sub>4</sub>MotB<sub>2</sub> stoichiometry was derived for the complex (51). This stoichiometry was used to calculate the numbers of stators per motor. Total internal reflection fluorescence microscopy of MotB labeled with green fluorescent protein (GFP–MotB) revealed 22 copies of GFP–MotB, which is consistent with 11 stators, each containing two MotB molecules. Interestingly, the fluorescence measurements disclosed diffusion of MotB in the membrane and rapid exchange with the motor (52). Such a dynamics may also apply for the ExbB–ExbD–TonB complex. The stable ExbB complex isolated and characterized in this work may represent the core on which the entire complex is assembled.

The structure of the ExbB–ExbD–TonB protein complex is a prerequisite to understand its way of function. As a first step, we isolated the most abundant protein of the complex, ExbB, from the cytoplasmic membrane and purified it to electrophoretic homogeneity. The protein was stable and formed a homooligomer with a defined shape and size. Since it was purified free of ExbD and TonB, we conclude that the oligomer is the basic core to which TonB and ExbD bind. During formation of the ExbB–ExbD–TonB complex additional ExbB monomers may be added to the heterooligomer.

## ACKNOWLEDGMENT

We gratefully acknowledge the beamtime allocation for the SAXS measurements at the European Synchrotron Radiation Facility, Grenoble, France, and the technical assistance by Dr. Shirley Callow and the ESRF staff. We thank Andrei Lupas for generous support and Jürgen Berger for assistance in electron microscopy.

## REFERENCES

1. Braun, V., and Mahren, S. (2007) Transfer of energy and information across the periplasm in iron transport and regulation, in *The periplasm* (Ehrmann, M., Ed.) pp 276–286, ASM Press, Washington, DC.
2. Chu, B. C., Peacock, R. S., and Vogel, H. J. (2007) Bioinformatic analysis of the TonB protein family. *Biomaterials* 20, 467–483.
3. Postle, K., and Kadner, R. J. (2003) Touch and go: tying TonB to transport. *Mol. Microbiol.* 49, 869–882.
4. Postle, K., and Larsen, R. A. (2007) TonB-dependent energy transduction between outer and cytoplasmic membranes. *Biomaterials* 20, 453–465.
5. Schauer, K., Rodionov, D. A., and de Reuse, H. (2008) New substrates for TonB-dependent transport: do we only see the “tip of the iceberg”? *Trends Biochem. Sci.* 33, 330–338.

6. Kampfenkel, K., and Braun, V. (1993) Topology of the ExbB protein in the cytoplasmic membrane of *Escherichia coli*. *J. Biol. Chem.* *268*, 6050–6057.
7. Kampfenkel, K., and Braun, V. (1992) Membrane topology of the *Escherichia coli* ExbD protein. *J. Bacteriol.* *174*, 5485–5487.
8. Larsen, R. A., Letain, T. E., and Postle, K. (2003) *In vivo* evidence of TonB shuttling between the cytoplasmic and outer membrane in *Escherichia coli*. *Mol. Microbiol.* *49*, 211–218.
9. Pawelek, P. D., Croteau, N., Ng-Thow-Hing, C., Khursigara, C. M., Moiseeva, N., Allaire, M., and Coulton, J. W. (2006) Structure of TonB in complex with FhuA, *E. coli* outer membrane receptor. *Science* *312*, 1399–1402.
10. Shultis, D. D., Purdy, M. D., Banchs, C. N., and Wiener, M. C. (2006) Outer membrane active transport: structure of the BtuB:TonB complex. *Science* *312*, 1396–1399.
11. Fischer, E., Günter, K., and Braun, V. (1989) Involvement of ExbB and TonB in transport across the outer membrane of *Escherichia coli*: phenotypic complementation of *exb* mutants by overexpressed *tonB* and physical stabilization of TonB by ExbB. *J. Bacteriol.* *171*, 5127–5134.
12. Higgs, P. I., Larsen, R. A., and Postle, K. (2002) Quantification of known components of the *Escherichia coli* TonB energy transduction system: TonB, ExbB, ExbD and FepA. *Mol. Microbiol.* *44*, 271–281.
13. Karlsson, M., Hannavy, K., and Higgins, C. F. (1993) ExbB acts as a chaperone-like protein to stabilize TonB in the cytoplasm. *Mol. Microbiol.* *8*, 389–396.
14. Sauter, A., Howard, S. P., and Braun, V. (2003) *In vivo* evidence for TonB dimerization. *J. Bacteriol.* *185*, 5747–5754.
15. Ollis, A. A., Manning, M., Held, K. G., and Postle, K. (2009) Cytoplasmic membrane protonmotive force energizes periplasmic interactions between ExbD and TonB. *Mol. Microbiol.* *73*, 466–481.
16. Ghosh, J., and Postle, K. (2005) Disulphide trapping of an *in vivo* energy-dependent conformation of *Escherichia coli* TonB protein. *Mol. Microbiol.* *55*, 276–288.
17. Baba, T., Ara, T., Hasegawa, M., Takai, Y., Okumura, Y., Baba, M., Datsenko, K. A., Tomita, M., Wanner, B. L., and Mori, H. (2006) Construction of *Escherichia coli* K-12 in-frame, single-gene knockout mutants: the Keio collection. *Mol. Syst. Biol.* *2*, 0008.
18. Laemmli, U. K. (1970) Cleavage of structural proteins during the assembly of the head of bacteriophage T4. *Nature* *227*, 680–685.
19. Schagger, H., and von Jagow, G. (1991) Blue native electrophoresis for isolation of membrane protein complexes in enzymatically active form. *Anal. Biochem.* *199*, 223–231.
20. Morris, D. L. (1948) Quantitative determination of carbohydrates with Dreywood's anthrone reagent. *Science* *107*, 254–255.
21. Roe, J. H. (1955) The determination of sugar in blood and spinal fluid with anthrone reagent. *J. Biol. Chem.* *212*, 335–343.
22. Ianeselli, L., Zhang, F., Skoda, M. W., Jacobs, R. M., Martin, R. A., Callow, S., Prevost, S., and Schreiber, F. (2010) Protein-protein interactions in ovalbumin solutions studied by small-angle scattering: effect of ionic strength and the chemical nature of cations. *J. Phys. Chem. B* *114*, 3776–3783.
23. Zhang, F., Skoda, M. W., Jacobs, R. M., Martin, R. A., Martin, C. M., and Schreiber, F. (2007) Protein interactions studied by SAXS: effect of ionic strength and protein concentration for BSA in aqueous solutions. *J. Phys. Chem. B* *111*, 251–259.
24. Zhang, F., Skoda, M. W., Jacobs, R. M., Zorn, S., Martin, R. A., Martin, C. M., Clark, G. F., Weggler, S., Hildebrandt, A., Kohlbacher, O., and Schreiber, F. (2008) Reentrant condensation of proteins in solution induced by multivalent counterions. *Phys. Rev. Lett.* *101*, 148101.
25. Narayanan, T., Ed. (2008) Synchrotron small-angle X-ray scattering, Vol. II, Springer, Heidelberg.
26. Glatter, O., and Kratky, O., Eds. (1982) Small angle X-ray scattering, Academic Press, London.
27. Orthaber, D., Bergmann, A., and Glatter, O. (2000) SAXS experiments on absolute scale with Kratky systems using water as a secondary standard. *J. Appl. Crystallogr.* *33*, 218–225.
28. Konarev, P. V., Petoukhov, M. V., Volkov, V. V., and Svergun, D. I. (2006) ATSAS 2.1, a program package for small-angle scattering data analysis. *J. Appl. Crystallogr.* *39*, 277–286.
29. Guinier, A., and Fournet, G., Eds. (1955) Small angle scattering of X-rays, Wiley, New York.
30. Abramoff, M. D., Magelhaes, P. J., and Ram, S. J. (2004) Image processing with ImageJ. *Biophotonics Int.* *11*, 36–42.
31. Heuberger, E. H., Veenhoff, L. M., Duurkens, R. H., Friesen, R. H., and Poolman, B. (2002) Oligomeric state of membrane transport proteins analyzed with blue native electrophoresis and analytical ultracentrifugation. *J. Mol. Biol.* *317*, 591–600.
32. Klepsch, M., Schlegel, S., Wickstrom, D., Friso, G., van Wijk, K. J., Persson, J. O., de Gier, J. W., and Wagner, S. (2008) Immobilization of the first dimension in 2D blue native/SDS-PAGE allows the relative quantification of membrane proteomes. *Methods* *46*, 48–53.
33. Lasserre, J. P., Beyne, E., Pyndiah, S., Lapaillerie, D., Claverol, S., and Bonneau, M. (2006) A complexomic study of *Escherichia coli* using two-dimensional blue native/SDS polyacrylamide gel electrophoresis. *Electrophoresis* *27*, 3306–3321.
34. Wilkins, D. K., Grimshaw, S. B., Receveur, V., Dobson, C. M., Jones, J. A., and Smith, L. J. (1999) Hydrodynamic radii of native and denatured proteins measured by pulse field gradient NMR techniques. *Biochemistry* *38*, 16424–16431.
35. Gasteiger, E., Hoogland, C., Gattiker, A., Duvaud, S., Wilkins, M. R., Appel, R. D., and Bairoch, A. (2005) Protein identification and analysis tools on the ExpASY server, in *The Proteomics Protocols Handbook* (Walker, J. M., Ed.) pp 571–607, Humana Press, Totowa, NJ.
36. Alpes, H., Apell, H. J., Knoll, G., Plattner, H., and Riek, R. (1988) Reconstitution of Na<sup>+</sup>/K<sup>+</sup>-ATPase into phosphatidylcholine vesicles by dialysis of nonionic alkyl maltoside detergents. *Biochim. Biophys. Acta* *946*, 379–388.
37. Putnam, C. D., Hammel, M., Hura, G. L., and Tainer, J. A. (2007) X-ray solution scattering (SAXS) combined with crystallography and computation: defining accurate macromolecular structures, conformations and assemblies in solution. *Q. Rev. Biophys.* *40*, 191–285.
38. Petoukhov, M. V., Konarev, P. V., Kikhneya, A. G., and Svergun, D. I. (2007) ATSAS 2.1—towards automated and websupported small-angle scattering data analysis. *J. Appl. Crystallogr.* *40*, s223–s228.
39. Cohn, E. J., and Edsall, J. T. (1943) Density and apparent specific volume of proteins, in *Proteins, Amino Acids and Peptides* (Cohn, E. J., and Edsall, J. T., Eds.) Reinhold Publishing, New York.
40. Laue, T. M., Shah, B., Ridgeway, T. M., and Pelletier, S. L. (1992) Computer-aided interpretation of sedimentation data for proteins, in *Analytical Ultracentrifugation in Biochemistry and Polymer Science* (Harding, S. E., Horton, J. C., and Rowe, A. J., Eds.) pp 90–125, Royal Society of Chemistry, Cambridge.
41. Lipfert, J., Columbus, L., Chu, V. B., Lesley, S. A., and Doniach, S. (2007) Size and shape of detergent micelles determined by small-angle X-ray scattering. *J. Phys. Chem. B* *111*, 12427–12438.
42. Kline, S. (2006) Reduction and analysis of SANS and USANS data using IGOR Pro. *J. Appl. Crystallogr.* *39*, 895–900.
43. Ilavsky, J., and Jemian, P. R. (2009) Irena: tool suite for modeling and analysis of small-angle scattering. *J. Appl. Crystallogr.* *42*, 347–353.
44. Salvay, A. G., Santamaria, M., le Maire, M., and Ebel, C. (2007) Analytical ultracentrifugation sedimentation velocity for the characterization of detergent-solubilized membrane proteins Ca<sup>++</sup>-ATPase and ExbB. *J. Biol. Phys.* *33*, 399–419.
45. Cascales, E., Lloubes, R., and Sturgis, J. N. (2001) The TolQ-TolR proteins energize TolA and share homologies with the flagellar motor proteins MotA-MotB. *Mol. Microbiol.* *42*, 795–807.
46. Eick-Helmerich, K., and Braun, V. (1989) Import of biopolymers into *Escherichia coli*: nucleotide sequences of the *exbB* and *exbD* genes are homologous to those of the *tolQ* and *tolR* genes, respectively. *J. Bacteriol.* *171*, 5117–5126.
47. Kampfenkel, K., and Braun, V. (1993) Membrane topologies of the TolQ and TolR proteins of *Escherichia coli*: inactivation of TolQ by a missense mutation in the proposed first transmembrane segment. *J. Bacteriol.* *175*, 4485–4491.
48. Braun, V., and Herrmann, C. (1993) Evolutionary relationship of uptake systems for biopolymers in *Escherichia coli*: cross-complementation between the TonB-ExbB-ExbD and the TolA-TolQ-TolR proteins. *Mol. Microbiol.* *8*, 261–268.
49. Karlsson, M., Hannavy, K., and Higgins, C. F. (1993) A sequence-specific function for the N-terminal signal-like sequence of the TonB protein. *Mol. Microbiol.* *8*, 379–388.
50. Guihard, G., Boulanger, P., Benedetti, H., Lloubes, R., Besnard, M., and Letellier, L. (1994) Colicin A and the Tol proteins involved in its translocation are preferentially located in the contact sites between the inner and outer membranes of *Escherichia coli* cells. *J. Biol. Chem.* *269*, 5874–5880.
51. Kojima, S., and Blair, D. F. (2004) Solubilization and purification of the MotA/MotB complex of *Escherichia coli*. *Biochemistry* *43*, 26–34.
52. Leake, M. C., Chandler, J. H., Wadhams, G. H., Bai, F., Berry, R. M., and Armitage, J. P. (2006) Stoichiometry and turnover in single, functioning membrane protein complexes. *Nature* *443*, 355–358.